Acta Biomaterialia 7 (2011) 4090–4101

Contents lists available at SciVerse ScienceDirect

Acta Biomaterialia

journal homepage: www.elsevier.com/locate/actabiomat

Dynamic mechanical response of brain tissue in indentation in vivo, in situ and in vitro

Thibault P. Prevost [a], Guang Jin [b], Marc A. de Moya [b], Hasan B. Alam [b], Subra Suresh [a], Simona Socrate [c,*]

[a] Department of Materials Science and Engineering, Massachusetts Institute of Technology, Cambridge, MA 02139, USA
[b] Department of Surgery, Division of Trauma, Emergency Surgery and Surgical Critical Care, Massachusetts General Hospital, Boston, MA 02114, USA
[c] Harvard-MIT Division of Health Sciences and Technology, Massachusetts Institute of Technology, Cambridge, MA 02139, USA

ARTICLE INFO

Article history:
Received 9 November 2010
Received in revised form 8 June 2011
Accepted 21 June 2011
Available online 25 June 2011

Keywords:
Brain indentation
Porcine
Viscoelasticity
Constitutive properties
Brain injury

ABSTRACT

Characterizing the dynamic mechanical properties of brain tissue is deemed important for developing a comprehensive knowledge of the mechanisms underlying brain injury. The results gathered to date on the tissue properties have been mostly obtained in vitro. Learning how these results might differ quantitatively from those encountered in vivo is a critical step towards the development of biofidelic brain models. The present study provides novel and unique experimental results on, and insights into, brain biorheology in vivo, in situ and in vitro, at large deformations, in the quasi-static and dynamic regimes. The nonlinear dynamic response of the cerebral cortex was measured in indentation on the exposed frontal and parietal lobes of anesthetized porcine subjects. Load–unload cycles were applied to the tissue surface at sinusoidal frequencies of 10, 1, 0.1 and 0.01 Hz. Ramp–relaxation tests were also conducted to assess the tissue viscoelastic behavior at longer times. After euthanasia, the indentation test sequences were repeated in situ on the exposed cortex maintained in its native configuration within the cranium. Mixed gray and white matter samples were subsequently excised from the superior cortex to be subjected to identical indentation test segments in vitro within 6–7 h post mortem. The main response features (e.g. nonlinearities, rate dependencies, hysteresis and conditioning) were measured and contrasted in vivo, in situ and in vitro. The indentation response was found to be significantly stiffer in situ than in vivo. The consistent, quantitative set of mechanical measurements thereby collected provides a preliminary experimental database, which may be used to support the development of constitutive models for the study of mechanically mediated pathways leading to traumatic brain injury.

1. Introduction

Traumatic brain injury (TBI) is a leading cause of death and morbidity in the developed world [1–6]. Understanding the precise mechanisms through which an external mechanical insult to the head translates into a local pattern of central nervous system (CNS) tissue/cell injury is acutely challenging. The challenge is daunting because the intricate combination of events suspected to result in TBI occurs at multiple levels: the macroscopic organ level, mesoscopic tissue level, microscopic cell level and nanoscopic molecular level. The multiplicity of scales mirrors the diversity of the physical processes involved. This diversity spans the traditional fields of science and engineering – from biophysics to medicine, mechanical engineering to biochemistry, and computer science to molecular biology. It may be hypothesized that TBI unfolds at the cell level, mainly as a consequence of the stress/strain constraints imposed on the CNS cells. A limited number of studies have been devoted to the investigations of the mechanical properties of single CNS cells [7,8]. Because the cell is a component of an organized tissue structure lying in a complex multi-organ system, how the loading transients imposed on the brain boundaries translate quantitatively into local traumatic tissue/cell strain–stress maps remains unclear. Quantifying the local mechanical impact of these transients on neural cell "assemblies" at the mesoscopic tissue level in ways that are both biologically relevant and mechanistically predictive calls for accurate biofidelic brain models to be developed – i.e. mechanical models that are able to capture the complexities of the tissue behavior in vivo. While the tissue response has been extensively characterized in vitro under various modes of deformation (e.g. shear [9–13], compression [14–19] and tension [16,20–22]), the availability of mechanical data on the living tissues remains limited. Three main experimental techniques have been employed to quantify brain tissue properties in vivo: magnetic resonance imaging elastography [23–28], surface suction [29] and indentation/local compression [30–34]. The first technique is noninvasive and may provide useful estimates of the tissue viscoelasticity in the linear

* Corresponding author. Tel.: +1 617 452 2689; fax: +1 617 258 8742.
E-mail address: ssocrate@mit.edu (S. Socrate).

1742-7061/$ - see front matter © 2011 Acta Materialia Inc. Published by Elsevier Ltd. All rights reserved.
doi:10.1016/j.actbio.2011.06.032

range at small levels of deformation. It relies, however, on calibration procedures and theoretical assumptions whose pertinence and accuracy are at times difficult to verify. The last two techniques are invasive but may provide direct measurements of tissue compliance. Indentation techniques especially have been widely used to characterize the mechanical response of biological tissues in their native state [35–40]. A few indentation studies have been conducted on the cortex of porcine brains in vitro [34,36,41], in situ [30,34,36] and in vivo [30–34]. Gefen and Margulies [34], in particular, led the largest scale in vivo study to date by measuring and comparing the relaxation response of 1 month old swine cortices in vivo and in situ via a 2 mm diameter indenter tip actuated to 4 mm depth on the exposed cortical surface at velocities of 1 and 3 mm s^{-1}. However, the complex features of the living brain large strain response – nonlinearities, hysteresis, rate dependencies – that are critical to developing comprehensive brain models have not been investigated thus far. The present study provides the first extensive set of experimental measurements carried out in vivo, in situ and in vitro on the superior cortex of porcine brains in an effort to assess and contrast the nonlinear dynamic indentation response of the cortex in its three physical states. The experiments detailed hereafter comprise measurements performed in indentation (cyclic load–unload and relaxation) on the frontal and parietal lobes of living and dead porcine brains with a 12.65 mm diameter hemispherical indenter, to 6 mm depth over a range of displacement rates spanning four orders of magnitude (0.12–120 mm s^{-1} velocities). The tests were conducted with a large-range dynamic indenter able to impose (in closed-loop motion control mode) sinusoidal displacements on the cortical surface to a penetration depth of 6 mm over a broad range of frequencies (0.01–10 Hz).

2. Materials and methods

2.1. Test apparatus

The indenting tool assembly (Fig. 1A) consisted of a voice coil linear actuator with a built-in LVDT displacement transducer (H2W Technologies Inc., Santa Clarita, CA) connected to a closed-loop motion control board (Galil Motion Control, Rocklin, CA). The voice coil shaft had an excursion amplitude of 38 mm and could operate in displacement-control mode at velocities up to ~120 mm s^{-1} (i.e. 10 Hz frequency for sinusoidal displacements of 6 mm). A 20 N load cell (Honeywell International Inc., Columbus, OH) was affixed to the voice coil shaft head in series with a 12.65 mm diameter hemispherical tip (Fig. 1B and C). As illustrated in Fig. 1C, the load sensor was located directly above the indenter tip to minimize inertial loading effects from the motion of the oscillating tool. Calibration tests were performed with the free indenter tip in air and the measured inertial force profiles were used to correct force profiles from tissue indentation tests. Effects of tool inertial loads were found to be discernible only at the highest testing frequency (10 Hz), while effects at lower rates were found to be negligible. The voice coil indenting assembly was mounted on a testing frame designed to accommodate large porcine animals in a setting mimicking conditions of an intensive care environment (Fig. 1A). The frame, characterized by six degrees of freedom in adjustable motion (i.e. three degrees in translation and three degrees in rotation), enabled the user to accurately position the indenter tip to the desired testing location and to align it normal to the measurement surface, as described elsewhere [42]. Briefly, its T-slotted aluminum structure (MiniTec Framing Systems LLC, Victor, NY) comprised two sets of linear rails allowing for manual

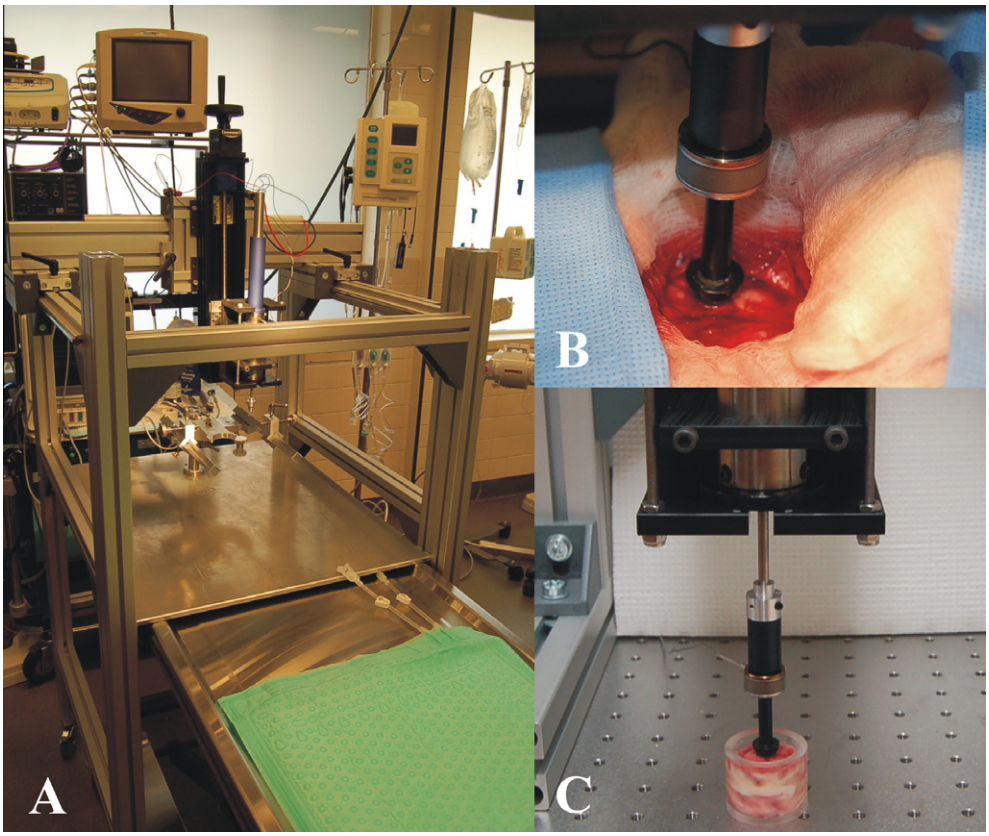

Fig. 1. Experimental setup. (A) Operating room configuration for the mechanical tests conducted in vivo and in situ. The stereotactic frame and the testing frame are shown along with the mechanical indenter and the BiSlide positioner. (B) Cranial window in vivo. The indenter tip affixed in series with the 20 N load cell is actuated on the exposed cortical lobes. (C) Testing configuration in vitro. The mechanical indenter is operated on the confined tissue bilayer excised from the superior part of the frontal and parietal lobes and maintained hydrated in PBS.

positioning adjustments in the horizontal plane along the x and y directions, respectively. Motion along the vertical z-axis was controlled via a manual BiSlide with counter (Velmex Inc., Bloomfield, NY), providing 250 mm of adjustable linear motion with 250 μm precision. A three-axis rotary stage connecting the portable indenter to the frame was attached to the BiSlide z-axis, providing ±25° of tilt from the vertical axis and 360° of rotation (Newport Corp., Irvine, CA).

Mechanical data sets (indenter force and displacement) were continuously acquired using two parallel acquisition systems: a low rate (~100 Hz) acquisition system integrated to the motion controller (Galil Motion Control, Rocklin, CA) and a higher rate (~5000 Hz) acquisition system for laptop-computer-based measurements (NI SC-2350 carrier and DAQCard-6036E with LabVIEW 8 software, National Instruments Corp., Austin, TX).

2.2. Surgical procedures

Five 3 month old Yorkshire pigs (42–45 kg) were used in this study, which comprised two distinct phases: an exploratory test phase on donor hemorrhaged animals (n = 2, male), during which the test protocols were developed, optimized and preliminary data were collected; and a full-scale test phase on nonhemorrhaged animals (n = 3, female), in which the optimized test protocols were

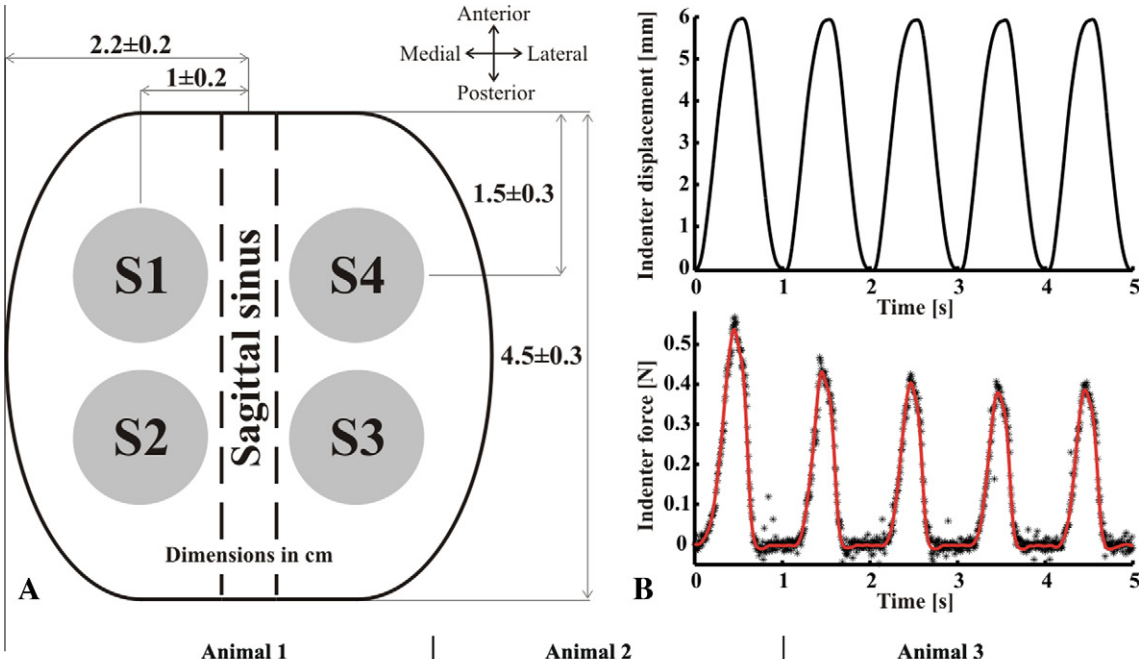

C

		Animal 1 Weight: 44 Kg			Animal 2 Weight: 45 Kg			Animal 3 Weight: 45 Kg		
		Time	Site	Test sequence	Time	Site	Test sequence	Time	Site	Test sequence
In vivo	3 hrs		1	M, L, Q, R		1	M, L, Q M, L, Q		1	M, L, Q, R M, F
			2	M, L, Q, L M, L, Q, F		4	F, M, L, Q		4	F, M
			3	M, L, Q, R F, M, L, Q		2	Q, M, L, F		1	M, L, Q, R
			2	F, M, L, Q, R					2	Q, M, L, F R, M
In situ		30 min	2	M, L, Q, R, F	30 min	2	M, L, Q, F	30 min	2	M, F, L, Q, R
		75 min	3	F, M, L, Q, R	70 min	4	M, L, Q, F	120 min	1	M, L, Q, F
		120 min	1	M, L, Q, F	120 min	1	F, M, L, Q	180 min	2	M, F
					180 min	4	Q, M, L, F			
In vitro		6.5 hrs		M, L, Q, R, F	7.5 hrs		M, L, Q, F M, L, R	6.5 hrs		M, L, Q, F M, L, Q, R

Fig. 2. Overview of indentation test protocols in vivo, in situ and in vitro. (A) Schematic of cranial window with localization of indentation sites S1, S2, S3 and S4. (B) Imposed indenter displacement history and resulting force history obtained for a representative set of measurements in vivo at a sinusoidal frequency of 1 Hz. The raw force profile (black dots) is shown superposed on the processed, smoothed profile (red solid line). (C) Summary of indentation tests conducted in vivo, in situ and in vitro on three nonhemorrhaged (3 month old female Yorkshire) animals. Cyclic test sequences to 6 mm depth are labeled as "F" (fast/10 Hz/120 mm s^{-1}), "M" (medium/1 Hz/12 mm s^{-1}), "L" (low/0.1 Hz/1.2 mm s^{-1}) and "Q" (quasistatic/0.01 Hz/0.12 mm s^{-1}). The 3 min relaxation tests with a ramp rate of 12 mm s^{-1} are labeled as "R". All cyclic tests corresponded to five load–unload sinusoidal segments and they were repeated at least twice except for the slowest cyclic tests (Q), which consisted of two or three load–unload segments performed only once. The times indicated for in situ and in vitro test sequences refer to post-mortem times.

implemented. All procedures were approved by the relevant institutional committees at the Massachusetts General Hospital, where the in vivo and in situ tests were carried out, and at the Massachusetts Institute of Technology, where the in vitro tests were conducted. The protocols were also approved by the animal care and use committee of the funding agency (US Department of Defense).

The animals were housed in the animal care facility for at least 4 days before experiment and allowed free access to food and water until 12 h before induction of anesthesia. Anesthesia was induced via intramuscular injection of 4.4 mg kg^{-1} of Telazol (tiletamine hydrochloride + zolazepam hydrochloride, Fort Dodge Animal Health, Fort Dodge, IA). The animals were intubated via an endotracheal tube connected to a ventilator with isoflurane general anesthesia and controlled mechanical ventilation. After intubation, anesthesia was maintained with 1.5–2% isoflurane. Body temperature was maintained using a heating pad preset at 37 ± 0.5 °C.

Physiological saline solution was administered intravenously at a maintenance infusion rate of 5 ml kg^{-1} h^{-1} throughout the test procedure. Prior to surgery, the head of the pig was secured in a stereotactic frame, adapted from previous design developments [43], with skull pegs affixed to the zygoma to prevent movement of the cranium (Fig. 1A). Hemorrhaged animals were fully resuscitated with saline solution (0.9% NaCl: three times the volume of shed blood) to replace the blood loss. The scalp was reflected off the cranium via a midline scalp incision, and a craniotomy was performed with a hand-held drill, exposing the superior part of both cortical hemispheres through a cranial window that was approximately 4.5 cm × 4.5 cm in size (Fig. 2A). The dura mater was carefully reflected to allow for direct mechanical measurements on the cortical surface. Physiological/hemodynamic parameters (heart rate, respiratory rate, blood pressure, end-tidal carbon dioxide, hemoglobin saturation level and body temperature) were monitored every 5 min for the entire duration of the test procedure, which lasted about 5 h (from sedation to euthanasia). The average values of these physiological parameters are listed in Table 1. After completion of the in vivo tests, the subjects were euthanized with an intravenous injection of Ethasol (0.25 ml kg^{-1}).

2.3. Indentation tests

The indenter was equipped with a 12.65 mm diameter hemispherical tip. Indentation tests were conducted in vivo on the frontal and parietal lobes of both hemispheres at four distinct sites located ~1.5 cm from the craniotomy edges (Fig. 2A). Test sequences consisted of 2–5 load–unload cycles to 6 mm indentation depth at sinusoidal frequencies of 10, 1, 0.1 or 0.01 Hz, corresponding to average displacement rates of 120, 12, 1.2 or 0.12 mm s^{-1}, respectively (see e.g. Fig. 2B). Tests were also performed to measure tissue relaxation response, with loading ramps at 12 mm s^{-1} to a target indentation depth of 6 mm and holding times of 180 s. The tissue was allowed to recover for 2 min between consecutive sequences of load–unload or relaxation segments. Tests at a given site at a given frequency or speed were repeated at least twice, except for either those corresponding to the slowest (0.01 Hz) load–unload cycles or the relaxation segments, which were performed only once. After euthanasia, indentation tests were repeated in situ at the same sites 30–180 min post mortem. The brain was kept in its native configuration within the braincase throughout the in situ phase of the tests, and physiological saline solution was regularly added to the exposed surface to minimize tissue dehydration. The brain was subsequently removed from the cranium and transferred on ice to the laboratory for further testing in vitro. For the in vitro indentation tests, tissue specimens were placed in a 3 cm diameter × 2.8 cm height rigid cylindrical container (Fig. 1C). The tissue specimens consisted of ~2.5 cm thick tissue bilayers. The specimens were prepared by coring cylindrical samples measuring about 3 cm in diameter and 1.2 cm in height from the surface of the frontal and parietal lobes and layering them so as to bring both inferior faces into contact. This step was intended to minimize friction between the tissue specimens and the container, as the inferior surfaces of the cored samples were found to exhibit a higher proportion of (more adherent) white matter. The tissue was hydrated with refrigerated phosphate-buffered solution (PBS) to minimize friction with the walls of the container and to limit tissue degradation. Load–unload and relaxation sequences – identical to those conducted in vivo and in situ – were conducted in indentation on the confined tissue bilayer at 6–7 h post mortem. All tests in vitro were performed at room temperature ($T \sim 21$ °C). A summary of the optimized tests conducted in vivo, in situ and in vitro on the three nonhemorrhaged animals is provided in Fig. 2C.

Table 1
Physiological parameters monitored at 5 min intervals during the in vivo tests.

Parameter	Mean ± standard deviation
Heart rate (bpm)	101 ± 16
Respiratory rate (vpm)	10
Arterial pressure (mmHg)	97 ± 11 (systole)/43 ± 7 (diastole)
SpO_2 (%)	97.5 ± 0.5
Et-CO_2 (mmHg)	45.5 ± 3
Temperature (°C)	35.3 ± 0.6

Average values and standard deviations are provided for the nonhemorrhaged cases ($n = 3$).

2.4. Tissue contact – tapping protocol

Identifying contact between indenter tip and tissue in a reliable and reproducible manner is of critical importance in indentation tests, especially when using a spherical indenter tip and when measuring a tissue response that is nonlinear. Visual estimation of contact conditions was found to be imprecise and unreliable due to the presence of cerebrospinal fluid and blood surrounding the indentation sites. The contact determination procedure was further complicated in vivo by the brain surface oscillations stemming from respiratory perturbations and rhythmic blood pressure variations. For the initial tests carried out on hemorrhaged animals, contact between the indenter tip and tissue was established by visual inspection. With this visual inspection approach, substantial variability in the measured tissue response was noted, as shown for one representative set of measurements in Fig. 3A. This variability was assumed to arise mainly from uncertainties in the tissue contact determination procedure and therefore a more systematic determination method was developed. The latter entailed gently "tapping" the tissue surface down to 1 mm depth over a time span of 100 ms. The resulting contact force was measured and full contact was deemed to be established when the force differential associated with the 1 mm tapping test reached an amplitude of ~15–20 mN (Fig. 3B). The tapping method was found to drastically reduce the variability in the measured tissue response (Fig. 3C), and it was therefore systematically implemented for the subsequent tests conducted on nonhemorrhaged animals in vivo, in situ and in vitro. The vertical z-position of the indenter – as measured through the counter of the vertical BiSlide – was adjusted via the tapping method at the beginning of each indentation sequence. The adjusted position was carefully noted to assess any residual tissue deformation. When tests were performed on a previously indented site, a recovery period of at least 2 min was observed before the tapping procedure.

3. Results

All statistical analyses reported hereafter were based on one-way analysis of variance. Results were considered statistically significant at $p < 0.05$.

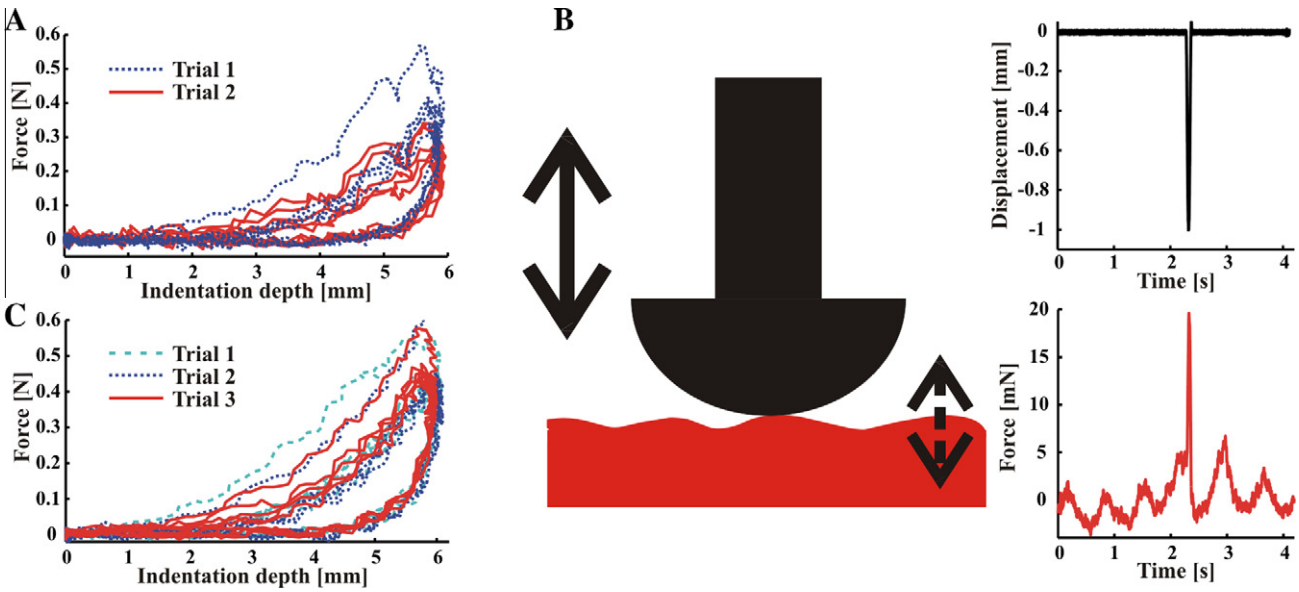

Fig. 3. Tissue contact/tapping protocol. (A) When contact was determined only by visual inspection, substantial variations in indenter force were observed between successive measurements. (B) Schematic of indenter tip position relative to oscillating tissue surface during contact determination procedure in vivo (left). Imposed tip displacement history and resulting force history measured for one representative case satisfying contact condition requirements (right). Note that the periodic force oscillations measured by the contacting tip corresponded to the brain surface movements associated with the ~100 bpm heart rate. (C) The proposed tapping protocol resulted in a reduction in response variability as shown for three successive measurements.

3.1. Preliminary observations – effect of dura mater on cortical tissue response

As part of the preliminary test phase involving the hemorrhaged animals, a small number of indentation experiments were carried out on the exposed cortex while leaving the dura mater intact. The tests were subsequently repeated at the same sites after the dura had been removed. The results are reported in Fig. 4 for one representative set of measurements. The response of the dura-free tissue was found to be significantly more compliant than that of the intact tissue. These observations remain qualitative in nature, as adhesion conditions of the dura membrane to the skull – which might be inferred to play a significant role in the indenter response – could not be accurately quantified. The observed trends were, however, consistent with expectations, since the dura mater had been shown to be a fairly stiff protective membrane with pseudo-elastic moduli measured in tension to be on the order of 60–100 MPa [44–46].

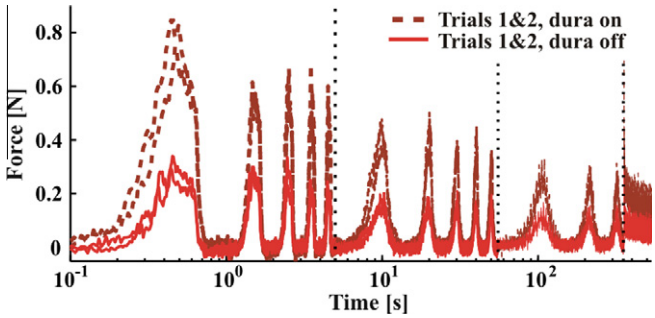

Fig. 4. Indenter force response shown for two representative sets of measurements performed while dura mater was left intact ($n = 2$) and subsequently removed ($n = 2$). Cyclic loading tests at 1, 0.1 and 0.01 Hz and relaxation tests are shown sequentially on the same time axis, although they were actually conducted as distinct test sequences separated by 2 min recovery phases.

3.2. Tissue recovery after indentation

The amount of residual tissue deformation observed after the 2 min recovery phase following each indentation sequence was measured in vivo, in situ and in vitro – via the *z*-counter of the vertical BiSlide – as the height differential applied to the indenter tip upon readjustment to contact with the tissue surface through the tapping protocol. A summary of the residual deformation results is provided in Table 2. The tissue was found to fully recover in vivo in most cases. After euthanasia, the exposed cortical surface was measured to shift downwards by 1.5 ± 0.1 mm over the 30 min period preceding the initiation of the indentation tests in situ. The tissue in situ never entirely recovered after a given indentation sequence; the amount of residual deformation measured between consecutive tests was on the order of 0.2–0.4 mm. Interestingly, the amount of residual deformation measured in vitro was substantially less than that in situ.

3.3. Test repeatability and rate order indifference

Representative responses measured during repeated tests conducted in vivo, in situ and in vitro at the same indentation sites to 6 mm depth at a displacement rate of 12 mm s^{-1} (1 Hz frequency) are shown in Fig. 5A–C. The responses to repeated indentation were found to be consistent and reproducible in vivo, as well as in situ and in vitro. To further assess the degree of repeatability in the mechanical measurements performed on a more quantitative basis, we compared the tissue responses to 1 Hz cyclic indentation in terms of peak force levels reached at the end of the first loading ramp for each sequence of load–unload segments applied to the tissue. These peak forces were compared within and across indentation sites according to four conditions: (I) the indentation site was not previously tested; (II) the indentation site was previously subjected to a minimum of one sequence of five load–unload segments at 1 Hz; (III) the indentation site was previously subjected to a minimum of one sequence of two-to-five load–unload segments at a lower indentation rate (i.e. 0.01 Hz and/or 0.1 Hz)

Table 2
Residual cortex surface deformation measured after 2 min recovery phase following indentation tests at 10, 1, 0.1 and 0.01 Hz in vivo, in situ and in vitro.

	Residual tissue indentation (mean ± SD) following cyclic loading test Dimensions in mm			
	10 Hz	1 Hz	0.1 Hz	0.01 Hz
In vivo	0.08 ± 0.1 (n = 8)	0.1 ± 0.2 (n = 22)	0.1 ± 0.2 (n = 12)	0.1 ± 0.1 (n = 11)
In situ	0.2 ± 0.2 (n = 12)	0.3 ± 0.3 (n = 12)	0.2 ± 0.15 (n = 9)	0.3 ± 0.2 (n = 13)
In vitro	0.05 ± 0.3 (n = 6)	0 ± 0.2 (n = 7)	0.15 ± 0.3 (n = 4)	0.15 ± 0.2 (n = 3)

Average values are provided with standard deviations for all tests performed on the three nonhemorrhaged animals.

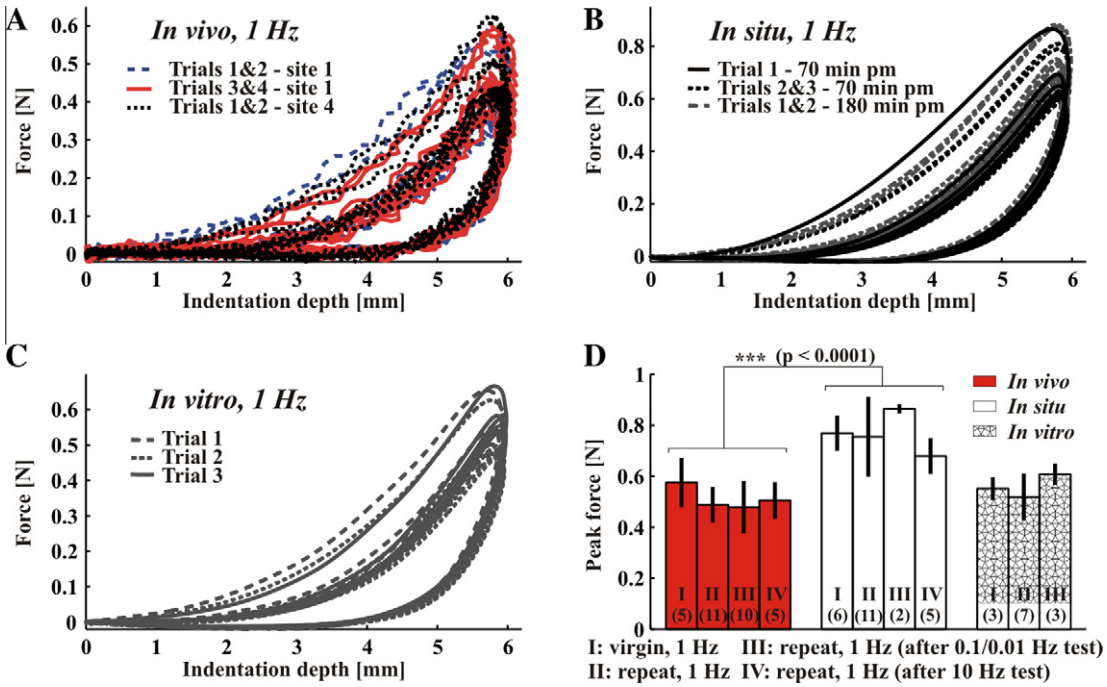

Fig. 5. Test repeatability in vivo, in situ and in vitro. (A) Representative indentation responses measured in vivo during repeated loading at 1 Hz. (B) Representative indentation responses measured in situ on the same site during repeated trials at various times post mortem (pm). (C) Representative indentation responses measured in vitro for three successive trials. (D) Peak forces reached at the end of the first loading ramp in vivo, in situ and in vitro across four conditions. Responses measured in vitro under condition III corresponded to 1 Hz tests repeated after both lower rate (0.01 Hz/0.1 Hz) and faster rate (10 Hz) tests had been conducted. Numbers in parentheses correspond to numbers of measurements performed under each condition for a total of three nonhemorrhaged animals. The response was found to be significantly stiffer in situ than in vivo ($p < 10^{-4}$).

with no prior submission to higher rate (i.e. 10 Hz) indentation sequences; and (IV) the indentation site was previously subjected to at least one sequence of five load–unload segments at higher indentation rate (i.e. 10 Hz) with no prior submission to lower rate (i.e. 0.01 Hz and/or 0.1 Hz) indentation sequences. The results are shown in Fig. 5D. Although the responses measured on virgin (previously untested) sites in the in vivo, in situ and in vitro states were found to be somewhat stiffer than those obtained on previously tested sites, these differences did not reach statistical significance ($p > 0.05$ for all cases compared individually to the virgin case). These observations suggest that precompressing the tissue or altering the rate order in vivo, in situ or in vitro does not significantly influence subsequent measurements (provided that the tissue is allowed to recover for at least 2 min between tests, tissue hydration conditions are maintained and proper contact is ensured at the beginning of each test sequence). All measurements reported hereafter for a given displacement rate were therefore averaged regardless of the indentation sequence order.

3.4. Location dependence

Repeated measurements performed in vivo at 1 Hz were compared quantitatively across indentation sites in terms of peak force levels reached at the end of the first (unconditioned) loading ramp and the second (conditioned) loading ramp. The results are reported in Fig. 6. The response of the tissue was found to be weakly dependent on indentation site. Although obtained from a fairly small pool of measurements, these results suggest that the frontal and parietal lobes of the superior cortex share similar mechanical properties at the macroscopic level. All measurements reported hereafter were therefore averaged across indentation sites.

3.5. Post mortem time differences

The effects of post-mortem test time on indentation response were also investigated in situ, as shown in Figs. 5B and 7. No statistically significant changes in relation to post-mortem time

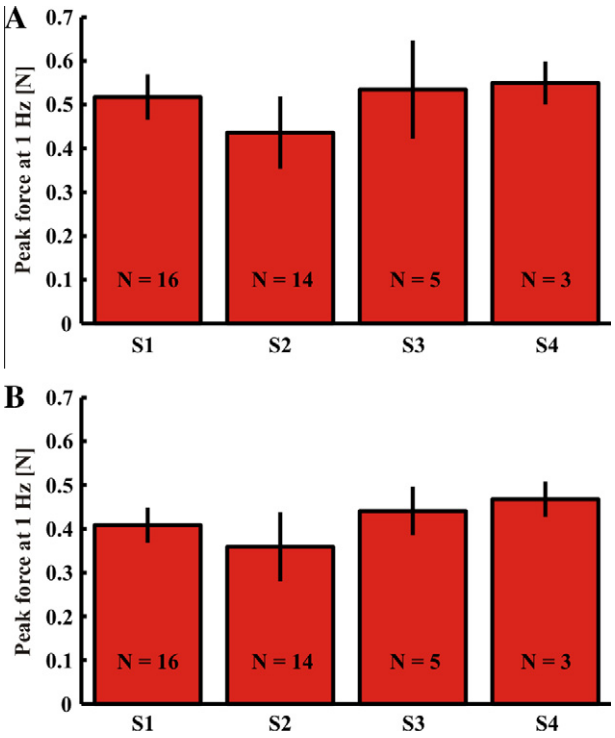

Fig. 6. Test location dependence. Peak forces measured at the end of the first loading ramp (unconditioned response, A) and at the end of the second loading ramp (conditioned response, B) for the four indentation sites submitted to 1 Hz load–unload cycles in vivo. *N* refers to the number of independent measurements performed on the three nonhemorrhaged animals.

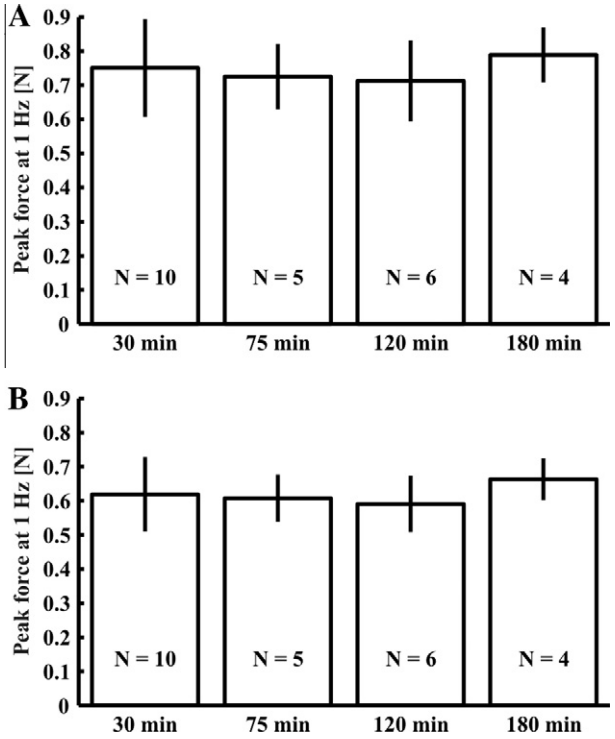

Fig. 7. Post mortem time variations in situ. Peak forces measured at the end of the first loading ramp (unconditioned response, A) and at the end of the second loading ramp (conditioned response, B) at various times post mortem. *N* refers to the number of independent measurements performed on the three nonhemorrhaged animals.

differences (as measured via the peak forces reached at 6 mm depth upon first loading) could be found up to about 3 h post mortem for both the conditioned and unconditioned responses. Therefore, all measurements reported hereafter in situ were averaged across post-mortem test times.

3.6. Representative response in vivo

A representative set of indentation measurements conducted at 10, 1, 0.1 and 0.01 Hz to 6 mm depth in vivo is shown in Fig. 8. The force–displacement response was found to be highly nonlinear both in the displacement and displacement rate domains, with marked hysteretic features. Among other notable characteristics exhibited by the macroscopic indentation response in vivo was the substantial degree of "conditioning". Here "conditioning" means that the indentation response upon first loading, namely the "virgin" or "unconditioned" response, was measured to be significantly stiffer than that observed subsequently upon immediate cyclic reloading. These observations mirror those previously reported in vitro on cortical samples tested in uniaxial compression [15]. Note that the tissue recovered its "virgin" or "unconditioned" response when allowed to re-equilibrate for at least 2 min between tests (Fig. 5A).

3.7. Response in vivo compared to response in situ

Average responses (with standard deviations) are reported for load–unload and relaxation both in vivo and in situ in Fig. 9. The indentation response was measured to be stiffer in situ than in vivo, regardless of displacement rates. Differences in indentation responses between the in vivo and the in situ states were further assessed quantitatively in terms of the peak forces measured upon first ("unconditioned") and second ("conditioned") loading, as shown in Fig. 9F. Differences were especially marked at low-to-quasistatic displacement rates, for which the indentation response was found to be stiffer in situ than in vivo by a factor of 1.5–2. These differences became more attenuated at higher displacement rates, as statistical differences grew smaller (Fig. 9F).

3.8. Response in situ compared to response in vitro

The indentation response in vitro was found to be more "compliant" than that measured in situ, with peak forces being on average 20% lower in vitro (Fig. 10). These differences might be ascribed to boundary condition effects and/or to intrinsic material property changes due to temperature variations and/or tissue alteration in relation to post-mortem testing time.

3.9. Nonlinear rate dependencies

The indentation response was measured to be highly rate dependent in vivo, in situ and in vitro (Fig. 10). These differences were also statistically significant as measured by the peak forces reached at 6 mm penetration depth ($p < 0.05$ when comparing pairs of peak forces between consecutive rates in vivo, in situ and in vitro). Note that the sensitivity of the indentation response to displacement rate grew higher, in relative terms, as displacement rates increased. In vivo, as shown in Fig. 10, peak forces at 10 Hz exceeded those measured at 1 Hz by a factor of 2.5, whereas peak forces at 0.1 Hz exceeded those reached at 0.01 Hz only by a factor of 1.5.

3.10. Conditioning effects

Conditioning effects – as measured by the ratio of the peak force upon reloading (conditioned response) to that reached upon first

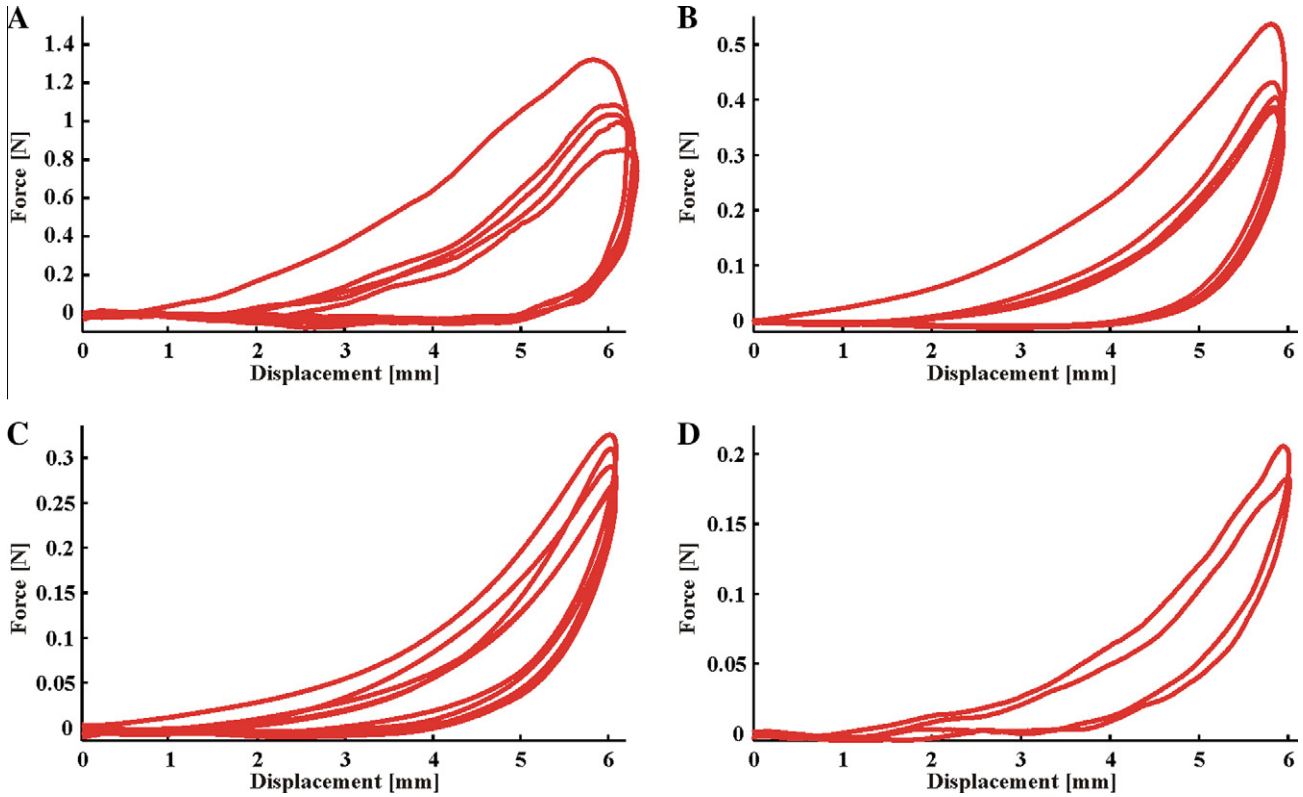

Fig. 8. Representative indentation response measured in vivo at 10 Hz (A), 1 Hz (B), 0.1 Hz (C) and 0.01 Hz (D). Periodic perturbations arising from respiratory movements and blood pressure pulsations (Fig. 3B and 5A) were filtered to yield the shown smoothed force–displacement profiles.

loading (unconditioned) – were found to be substantial in vivo, in situ and in vitro (Fig. 10). Note that these conditioning effects tended to be more attenuated at lower rates of deformation, with conditioning ratios in vivo reaching 0.9 ± 0.03 on average at quasi-static rates (0.01 Hz), compared to 0.8 ± 0.05 at higher rates (10 Hz).

3.11. Comparison with literature data

Brain indentation measurements in vivo and in situ were reported previously by Gefen and Margulies at quasistatic displacement rates (1–3 mm s^{-1}) [34]. Their data cannot be directly compared to the data collected in the present study due to differences in indenter tip radius (2 vs. 6.3 mm) and maximum indentation depth (4 vs. 6 mm). However, when the indentation forces at 4 mm depth were simply normalized by the ratio of nominal cross-sectional areas of the tips (square of the radii), the data obtained in the present study were found to be comparable to those reported by Gefen and Margulies, both for the unconditioned and conditioned responses (Fig. 11). Note, however, that the definition for "conditioned response" somewhat differed between the two protocols. "Conditioned response" in the protocol by Gefen and Margulies referred to the combined fifth and sixth single loading ramps applied to the tissue as part of a series of six single ramp relaxation tests separated by 45 s recovery phases. On the other hand, data selected for comparison from the present study corresponded to the fifth (and last) loading ramp imposed on the tissue as part of a single sequence of five continuously applied load–unload segments. Also note that the investigation led by Gefen and Margulies was conducted on younger porcine animals (i.e. 1 month of age), whose brain properties in vitro have been shown to be comparable to those of adult pigs [47]. As previously mentioned, rate effects were found to be more significant at the higher frequencies in vivo, in situ and in vitro. This trend is in good agreement with the results of previous investigations, where brain tissue response was found to dramatically stiffen at higher rates of deformation [17,22,48].

4. Discussion

The present study reports the first body of observations on the indentation response of porcine cerebral cortex at quasistatic and dynamic deformation rates in vivo. The set of measurements conducted addresses previously uncharacterized features of the living porcine cerebral cortex mechanical response to large deformations (6 mm indentation depth) and over a broad range of displacement rates (0.12–120 mm s^{-1}). These features have been directly contrasted with those characterizing the indentation response in situ and in vitro, thereby providing a unique quantitative basis for further refinements/adjustments of existing biomechanical models relying so far on experimental sets of in vitro and in situ measurements.

The preliminary experiments carried out on two hemorrhaged pigs allowed for rigorous test protocols to be developed, minimizing measurement variability via implementation of more systematic contact determination procedures. The data sets subsequently collected on three nonhemorrhaged animals in vivo and in situ were found to be consistent and comparable with those reported by previous investigators at smaller indentation depths and lower rates of deformation [34]. The tissue in vivo was observed to recover fully after a 2 min recovery phase following each cyclic loading test. Some residual deformation was noted in situ after indentation. The dependence of the load–displacement response on the indentation site was found to be weak, thereby confirming cerebral tissue mechanical homogeneity at the macroscopic level on the frontal and parietal lobes [34,49].

The indentation response was observed to share highly similar patterns in vivo, in situ and in vitro – e.g. conditioning, time/rate

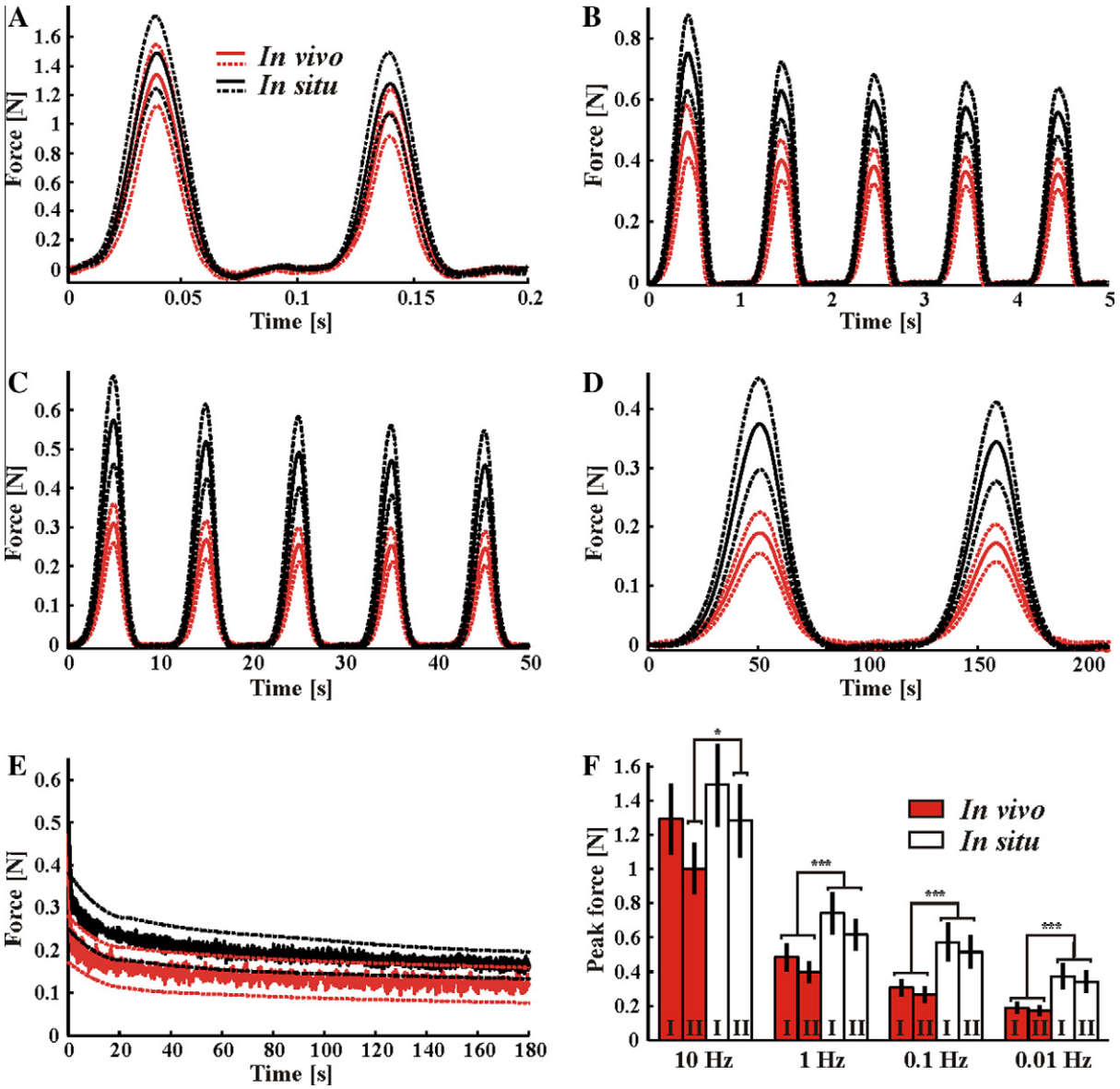

Fig. 9. Indentation responses contrasted in vivo and in situ in cyclic load–unload at 10 Hz (A), 1 Hz (B), 0.1 Hz (C) and 0.01 Hz (D), and in relaxation (E). Average responses (solid lines) and average responses plus or minus standard deviations (dashed lines) are shown in each case. For clarity purposes, only the first two load–unload cycles are shown in the 10 Hz case. (F) Response in vivo compared to response in situ in terms of peak forces reached at the end of the first loading ramp (I) and of the second loading ramp (II) for the four different rates of deformation. *Significant ($p < 0.05$) and ***very significant ($p < 10^{-4}$) statistical differences.

dependencies, nonlinear indentation depth dependencies. These patterns are consistent with the inherent properties exhibited by porcine brain tissue when tested in vitro in unconfined compression and in uniaxial tension [15,16,19].

Conditioning effects were found to be significant in vivo, in situ and in vitro. These effects could be recovered when allowing the tissue to re-equilibrate for 2 min. These observations confirm preliminary findings in vitro where precompressed tissue samples were shown to exhibit repeatable conditioning features following a 2 h recovery phase in saline solution [15]. These conditioning effects might be ascribed to interstitial water diffusion within the tissue as surmised earlier [15]. The latter inference is consistent with the fact that the amount of conditioning measured in the present study was found to be rate dependent, with more substantial conditioning effects observed at higher rates of deformation.

The brain was measured to shrink/settle following euthanasia, descending by 1.5 ± 0.1 mm ($n = 3$ animals) at the exposed cortical surface, suggesting that the organ might undergo some degree of "consolidation" post mortem. Possible factors governing the consolidation process conjectured post mortem include: (i) the collapse of the tissue vasculature; and (ii) drainage of cerebrospinal fluid (CSF)-filled cavities (e.g. ventricles, sinuses).

The indentation response was measured to be significantly stiffer in situ than in vivo. This important observation only partially agrees with the previous findings by Gefen and Margulies [34], who reported increased stiffness for the nonconditioned response only, although the latter increase was found not to be statistically significant. Differences between in situ and in vivo indentation responses might also be enhanced in the current study due to the larger indenter size and indentation depth, although the indenter radius for the current study is still within the general guidelines recommended by Zheng et al. [50] for tissue characterization (~25% of the sample thickness). Also, the effects of drainage of the internal CSF cavities and the observed downward shift of tissue surface might be more pronounced in the current study, where larger regions of the brain are deformed by the applied surface indentation. Note, however, that the measured tissue shift post mortem, although significant, remains small relative to the overall thickness of the cerebrum within

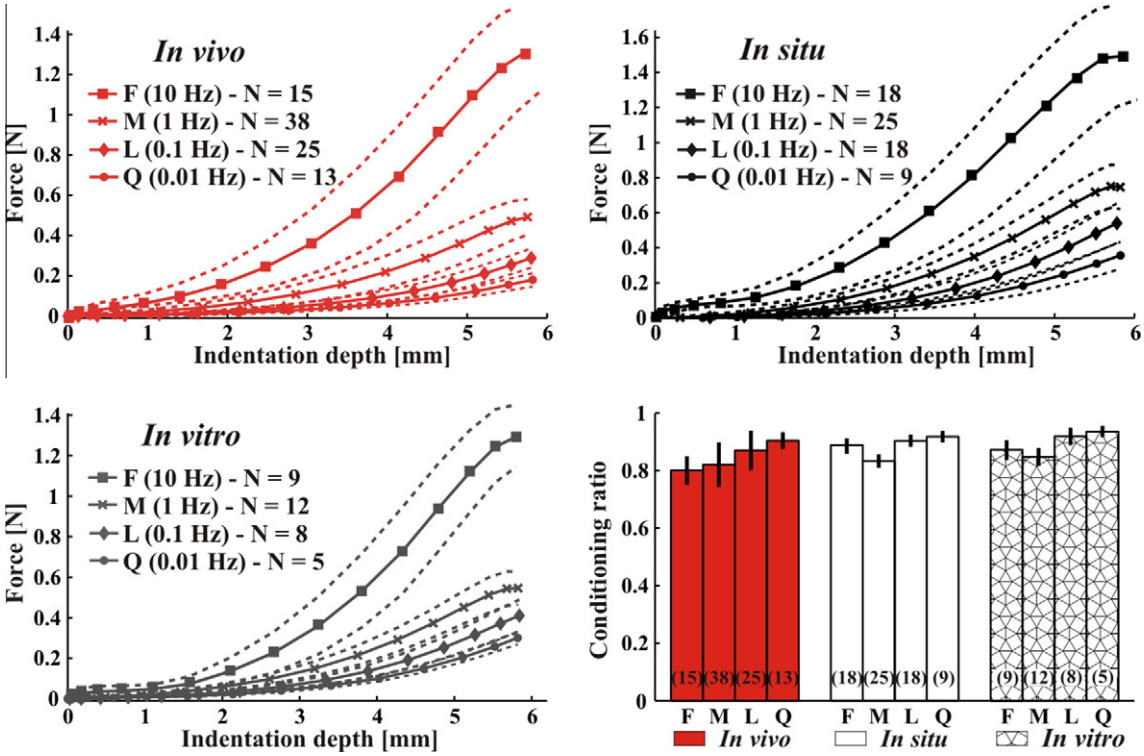

Fig. 10. Average indentation response upon first cyclic loading in vivo, in situ and in vitro. Dashed lines correspond to average plus or minus standard deviation. Conditioning ratios (bottom right) are also shown for each deformation rate (F, M, L, Q) in vivo, in situ and in vitro. The conditioning ratio is defined as the ratio between the peak forces reached at the end of the second loading ramp (conditioned) and the peak forces reached at the end of the first loading ramp (unconditioned).

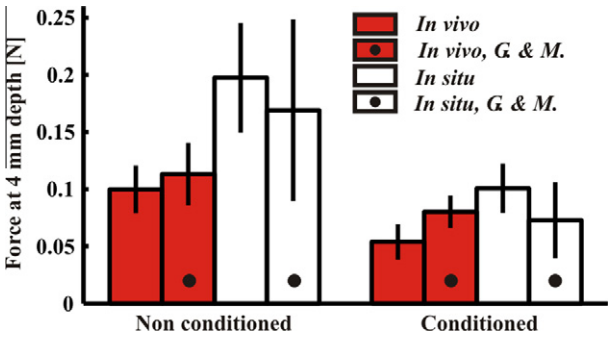

Fig. 11. Comparison of results obtained under the current protocol and under the protocol developed by Gefen and Margulies [34]. Average peak forces at 4 mm depth (with standard deviations) are shown for the nonconditioned and conditioned responses measured in vivo and in situ. Force levels from Ref. [34] were normalized by the ratio between nominal cross sectional areas of the indenters for direct comparison with the force data collected in the present study.

the braincase (which was typically about 25 mm), so that possible stiffening artifacts arising from depth alteration effects alone are unlikely to account for the observed changes in indenter force magnitude. Other factors that might contribute to the observed increase in stiffness include alterations to the intrinsic mechanical properties of the structural components responsible for the neural cell resilience (i.e. actin filaments, neurofilaments and microtubules), and tissue edema. Other investigators have reported similar changes in material properties between the in vivo and in situ states in "cellular" and highly vascularized organs such as liver [40].

Finally, results gathered in vitro were also reported. The force–displacement response was found to be more compliant than the response measured in situ. This difference might be ascribed to alterations in tissue properties due to temperature changes and/or intrinsic tissue degradation post mortem, or to boundary condition effects. Variations in tissue properties related to post-mortem degradation processes were found to be negligible up to 15 h post mortem by several investigators [15,51], while some differences were noted by others beyond 6 h post mortem [52]. Temperature variations between the in situ and in vitro tests may have played a role in the reported changes in tissue response. Note, however, that temperature effects, if substantial, should have increased the tissue stiffness in vitro, as was reported when the test temperature had been lowered [53]. It is therefore very plausible that material property alterations due to intrinsic tissue degradation and/or temperature changes alone could not account for the substantial differences noted in the measurements between the in situ and in vitro states, and that boundary condition effects played a significant role.

This consideration highlights one of the restrictions of the present study, which was limited to the macroscopic force–displacement response to brain cortex indentation. The nonlinear characteristics of the indentation response could be ascribed to a combination of intrinsic material (brain tissue) nonlinearities and boundary conditions effects related to the complex deformation field associated with indentation tests, as well as to the constraints provided by the braincase (or by the cylindrical container employed for in vitro tests). Reverse finite element modeling is therefore needed to gain better insights into the effects of boundary conditions on the resulting force–indentation response and extract tissue properties from the measured indentation responses. Finite element modeling of the precise testing conditions will also provide a direct means to compare and reconcile the in situ and in vitro responses. As a further limitation of the present study, it should be noted that the data pool harvested was obtained from three animals only. Although very consistent, the measurements reported would need to be complemented by further testing. Finally, the indentation technique employed was limited to single

uniaxial force–displacement measurements. Complementary techniques relying on the use of peripheral secondary sensors around the locus of indentation may provide useful additional information to the tissue volumetric compliance described elsewhere [54].

Taken together, the sets of experimental data presented here provide unique insights into the dynamic mechanical response of cerebral cortex to indentation both in vivo and in situ, and may critically guide the development of biofidelic brain models. Additional mechanical data might also be obtained at higher rates of deformation using the current dynamic indenter, which is able to operate in open-loop mode at speeds as high as 4.5 m s^{-1}. The high-rate mechanical data that could be so collected in vivo, in situ and in vitro through open-loop "impact" tests might potentially lead to an improved understanding of the mechanical response of the brain under conditions approaching those suspected to prevail in blast or blunt impact traumatic brain injury scenarios.

Acknowledgements

This work was supported by the US Army Research Office and Joint Improvised Explosive Devices Defeat Organization, under Contract No. W911NF-07-1-0035; the US Army Medical Research Material Command GRANTT00521959 (to HBA); the MIT Institute for Soldier Nanotechnologies, under contract number W911NF-07-D-0004; École Nationale des Ponts et Chaussées (Université Paris-Est, France); the Computational Systems Biology Programme of the Singapore–MIT Alliance (SMA); and the Interdisciplinary Research Group on Infectious Diseases at the Singapore–MIT Alliance for Research and Technology (SMART). The authors are grateful to Dr. Asha Balakrishnan for designing the testing frame used in the in vivo experiments.

References

[1] Corrigan JD, Selassie AW, Orman JAL. The epidemiology of traumatic brain injury. J Head Trauma Rehabil 2010;25:72.
[2] Belanger HG, Kretzmer T, Yoash-Gantz R, Pickett T, Tupler LA. Cognitive sequelae of blast-related versus other mechanisms of brain trauma. J Int Neuropsychol Soc 2009;15:1.
[3] Crowe LM, Anderson V, Catroppa C, Babl FE. Head injuries related to sports and recreation activities in school-age children and adolescents: data from a referral centre in Victoria, Australia. Emerg Med Australas 2010;22:56.
[4] McCrory P, Makdissi M, Davis G, Collie A. Value of neuropsychological testing after head injuries in football. Br J Sports Med 2005;39:I58.
[5] Hoge CW, Goldberg HM, Castro CA. Care of war veterans with mild traumatic brain injury – flawed perspectives. N Engl J Med 2009;360:1588.
[6] Kraus JF, McArthur DL. Epidemiologic aspects of brain injury. Neurol Clin 1996;14:435.
[7] Lu YB, Franze K, Seifert G, Steinhauser C, Kirchhoff F, Wolburg H, et al. Viscoelastic properties of individual glial cells and neurons in the CNS. Proc Natl Acad Sci USA 2006;103:17759.
[8] Bernick KB, Prevost TP, Suresh S, Socrate S. Biomechanics of single cortical neurons. Acta Biomater 2011;7:1210.
[9] Shuck LZ, Advani SH. Rheological response of human brain tissue in shear. J Basic Eng 1972;94:905.
[10] Bilston LE, Liu ZZ, Phan-Thien N. Linear viscoelastic properties of bovine brain tissue in shear. Biorheology 1997;34:377.
[11] Darvish KK, Crandall JR. Nonlinear viscoelastic effects in oscillatory shear deformation of brain tissue. Med Eng Phys 2001;23:633.
[12] Nicolle S, Lounis M, Willinger R. Shear properties of brain tissue over a frequency range relevant for automotive impact situations: new experimental results. Stapp Car Crash J 2004;48:239.
[13] Hrapko M, van Dommelen JAW, Peters GWM, Wismans JSHM. The mechanical behaviour of brain tissue: large strain response and constitutive modelling. Biorheology 2006;43:623.
[14] Miller K, Chinzei K. Constitutive modelling of brain tissue: experiment and theory. J Biomech 1997;30:1115.
[15] Prevost TP, Balakrishnan A, Suresh S, Socrate S. Biomechanics of brain tissue. Acta Biomater 2011;7:83.
[16] Franceschini G, Bigoni D, Regitnig P, Holzapfel GA. Brain tissue deforms similarly to filled elastomers and follows consolidation theory. J Mech Phys Solids 2006;54:2592.
[17] Tamura A, Hayashi S, Watanabe I, Nagayama K, Matsumoto T. Mechanical characterization of brain tissue in high-rate compression. J Biomech Sci Eng 2007;2:115.
[18] Cheng S, Bilston LE. Unconfined compression of white matter. J Biomech 2007;40:117.
[19] Hrapko M, van Dommelen JAW, Peters GWM, Wismans JSHM. Characterisation of the mechanical behaviour of brain tissue in compression and shear. Biorheology 2008;45:663.
[20] Miller K, Chinzei K. Mechanical properties of brain tissue in tension. J Biomech 2002;35:483.
[21] Velardi F, Fraternali F, Angelillo M. Anisotropic constitutive equations and experimental tensile behavior of brain tissue. Biomech Model Mechanobiol 2006;5:53.
[22] Tamura A, Hayashi S, Nagayama K, Matsumoto T. Mechanical characterization of brain tissue in high-rate extension. J Biomech Sci Eng 2008;3:263.
[23] Muthupillai R, Lomas DJ, Rossman PJ, Greenleaf JF, Manduca A, Ehman RL. Magnetic resonance imaging of transverse acoustic strain waves. Science 1995;269:1854.
[24] McCracken PJ, Manduca A, Felmlee J, Ehman RL. Mechanical transient-based magnetic resonance elastography. Magn Reson Med 2005;53:628.
[25] Hamhaber U, Sack I, Papazoglou S, Rump J, Klatt D, Braun J. Three-dimensional analysis of shear wave propagation observed by in vivo magnetic resonance elastography of the brain. Acta Biomater 2007;3:127.
[26] Xu L, Lin Y, Han JC, Xi ZN, Shen H, Gao PY. Magnetic resonance elastography of brain tumors: preliminary results. Acta Radiol 2007;48:327.
[27] Atay SM, Kroenke CD, Sabet A, Bayly PV. Measurement of the dynamic shear modulus of mouse brain tissue in vivo by magnetic resonance elastography. J Biomech Eng – Trans ASME 2008;130:021013.
[28] Green MA, Bilston LE, Sinkus R. In vivo brain viscoelastic properties measured by magnetic resonance elastography. NMR Biomed 2008;21:755.
[29] Schiavone P, Chassat F, Boudou T, Promayon E, Valdivia F, Payan Y. In vivo measurement of human brain elasticity using a light aspiration device. Med Image Anal 2009;13:673.
[30] Metz H, McElhaney J, Ommaya AK. A comparison of the elasticity of live, dead, and fixed brain tissue. J Biomech 1970;3:453.
[31] Schettini A, Walsh EK. Brain tissue elastic behavior and experimental brain compression. Am J Physiol – Regul Integr Comp Physiol 1988;255:799.
[32] Miller K, Chinzei K, Orssengo G, Bednarz P. Mechanical properties of brain tissue in-vivo: experiment and computer simulation. J Biomech 2000;33:1369.
[33] Miga MI, Paulsen KD, Hoopes PJ, Kennedy FE, Hartov A, Roberts DW. In vivo modeling of interstitial pressure in the brain under surgical load using finite elements. J Biomech Eng – Trans ASME 2000;122:354.
[34] Gefen A, Margulies SS. Are in vivo and in situ brain tissues mechanically similar? J Biomech 2004;37:1339.
[35] Lai-Fook SJ, Wilson TA, Hyatt RE, Rodarte J. Elastic constants of inflated lobes of dog lungs. J Appl Physiol 1976;40:508.
[36] Gefen A, Gefen N, Zhu Q, Raghupathi R, Margulies SS. Age-dependent changes in material properties of the brain and braincase of the rat. J Neurotrauma 2003;20:1163.
[37] Vannah WM, Childress DS. Indentor tests and finite element modeling of bulk muscular tissue in vivo. J Rehabil Res Dev 1996;33:239.
[38] Gefen A, Megido-Ravid M, Azariah M, Itzchak Y, Arcan M. Integration of plantar soft tissue stiffness measurements in routine MRI of the diabetic foot. Clin Biomech 2001;16:921.
[39] Li LP, Herzog W. Arthroscopic evaluation of cartilage degeneration using indentation testing – influence of indenter geometry. Clin Biomech 2006;21:420.
[40] Kerdok AE, Ottensmeyer MP, Howe RD. Effects of perfusion on the viscoelastic characteristics of liver. J Biomech 2006;39:2221.
[41] van Dommelen JAW, van der Sande TPJ, Hrapko M, Peters GWM. Mechanical properties of brain tissue by indentation: interregional variation. J Mech Behav Biomed Mater 2010;3:158.
[42] Balakrishnan A. Development of novel dynamic indentation techniques for soft tissue applications. PhD thesis, Massachusetts Institute of Technology; 2007.
[43] Manley GT, Rosenthal G, Lam M, Morabito D, Yan DH, Derugin N, et al. Controlled cortical impact in swine: pathophysiology and biomechanics. J Neurotrauma 2006;23:128.
[44] McGarvey KA, Lee JM, Boughner DR. Mechanical suitability of glycerol-preserved human dura mater for construction of prosthetic cardiac valves. Biomaterials 1984;5:109.
[45] Runza M, Pietrabissa R, Mantero S, Albani A, Quaglini V, Contro R. Lumbar dura mater biomechanics: experimental characterization and scanning electron microscopy observations. Anesth Analg 1999;88:1317.
[46] Maikos JT, Elias RAI, Shreiber DI. Mechanical properties of dura mater from the rat brain and spinal cord. J Neurotrauma 2008;25:38.
[47] Prange MT, Margulies SS. Regional, directional, and age-dependent properties of the brain undergoing large deformation. J Biomech Eng – Trans ASME 2002;124:244.
[48] Pervin F, Chen WW. Dynamic mechanical response of bovine gray matter and white matter brain tissues under compression. J Biomech 2009;42:731.
[49] Coats B, Margulies SS. Material properties of porcine parietal cortex. J Biomech 2006;39:2521.
[50] Zheng YP, Mak AFT, Lue B. Objective assessment of limb tissue elasticity: development of a manual indentation procedure. J Rehabil Res Dev 1999;36:71.

[51] McElhaney JH, Melvin JW, Roberts VL, Portnoy HD. Dynamic characteristics of the tissues of the head. In: Kenedi RM, editors. Perspectives in biomedical engineering. London: The MacMillan Press Ltd.; 1973. p. 215.
[52] Garo A, Hrapko M, van Dommelen JAW, Peters GWM. Towards a reliable characterisation of the mechanical behaviour of brain tissue: the effects of post-mortem time and sample preparation. Biorheology 2007;44:51.
[53] Hrapko M, van Dommelen JAW, Peters GWM, Wismans JSHM. The influence of test conditions on characterization of the mechanical properties of brain tissue. J Biomech Eng – Trans ASME 2008;130:031003.
[54] Balakrishnan A, Socrate S. Material property differentiation in indentation testing using secondary sensors. Exp Mech 2008;48:549.